# Experimental Application of a Pragmatic Method to Design Control Strategy for Low Power Wind Energy Conversion System

Radu Boraci and Cristian Vasar

"Politehnica" University of Timisoara/
Department of Automation and Applied Informatics, Romania
{radu.boraci,cristian.vasar}@aut.upt.ro

**Abstract.** This paper proposes a method for designing, implementation and experimental validation of a control strategy dedicated to a low power wind generator. It was developed theoretically then applied to a low speed wind generator prototype. The proposed wind energy conversion system control structure is briefly described, including its subsystems and components, respectively the wind turbine, permanent magnets synchronous generator, electronic converters and brake system. There were taken into consideration the components characteristics determined theoretically and experimentally obtained from components manufacturers or a dedicated laboratory model. The control law for the optimal operation regime of the wind turbine was designed considering the wind speed and the individual characteristics of the wind energy conversion system components and their operating restrictions. Also, there were determined the start and stop conditions, the allowed turbine speed ranges and the consequent braking regimes. Simulation and experimental results demonstrate the effectiveness of the proposed approach.

**Keywords:** small windmills, wind turbines, magnet poles synchronous generators, windgenerator electronics, braking systems, control methods and algorithms.

## 1 Introduction

During last decades, the interest for renewable energy technologies increased both for scientists and the industrial environment. In this field, a special place is taken by the wind energy conversion systems (WECSs). The control strategies used to convert wind into electricity covers a broad range, from those based on constant speed to the advanced ones for variable speed supported by electronic converters, for on-grid or off-grid WECSs [1,2] .

An important demand can be noticed on the market for low speed wind generators (1 to 10 KW), operating in locations with various wind profiles. Most of these WECSs are based on wind turbines with non-regulated blades and permanent magnet synchronous generators functioning at variable speed to optimize the power extracted

V.E. Balas et al. (Eds.): Soft Computing Applications, AISC 195, pp. 183–195.
springerlink.com 

from wind. They are interfaced with consumers or grid using static electronic converters with variable frequency and voltage for input and constant frequency and voltage for output.

One experimental setup for a low power WECS (presented in figure 1) was developed by Politehnica University of Timisoara, in the frame of the European Economic Area Grant "Improvement of the structure and efficiency of small horizontal axis wind generators with non-regulated blades.

**Fig. 1.** Experimental windgenerator

The WECS components were developed, implemented, studied and optimized considering the actual trends in this field.

## 2 WECS Components

### 2.1 Wind Turbine

One important component of the presented system is the wind turbine. The blades are twisted in space, with metal insertion and variable geometry. They are equipped with

flaps for noise reduction and finite span effect that requires a special study to find the optimal control solution.

A special requirement for the wind turbine was to be able to provide energy even at low wind speed. This condition lead to the necessity to limit the rotation speed at higher wind speeds. Thus it was developed a protection mechanism to adapt the blade stall in order to adjust the turbine aerodynamic characteristics, limiting the power extracted from wind and the rotation speed.

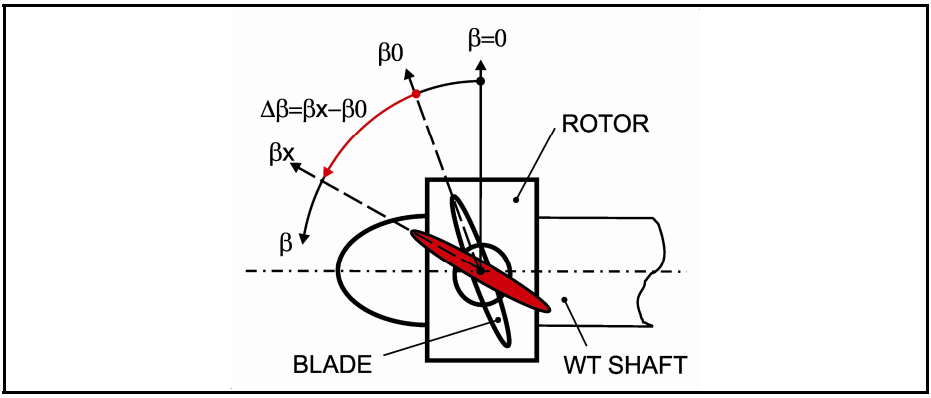


**Fig. 2.** The rotor of wind turbine

The rotor of wind turbine is presented in Figure 2.The blade absolute position is defined by the $\beta_x$ angle. In normal operation, when the limitation system is not active, the blades angle is $\beta_0$.

The relative position of the blade is

$$\Delta\beta = \beta_x - \beta_0 \, , \, \Delta\beta = 0 \ldots 45 \text{ dgr.} \tag{1}$$

The manufacturing procedure was based on fiberglass reinforced polyester for obtaining products with a complex structure [3] .

## 2.2 Permanent Magnet Synchronous Generator

Based on the wind turbine estimated characteristics and existing statistical data, there resulted the following rated values for designing the permanent magnet synchronous generator (PMSG): $(P_{PMSG})_{rated}$ = 5400W, $(n_{PMSG})_{rated}$ = 122 rpm.

The PMS generator integrates a electromechanical brake and was manufactured by S.C. BEGAELECTROMOTOR S.A. Timişoara, România. The actual physical parameters were determined through experimental tests in the laboratory as follows for cosφ = 1:

$P_{rated}$ = 6075 W - rated power;
$U_{rated}$ = 162 V - rated phase voltage;
$I_{rated}$ = 12.5 A - rated phase current;
$M_{rated}$ = 484 N m - rated torque;
$\eta_{rated}$ = 0,91 - rated efficiency;
$\Phi_{f0}$ = 1,42 Wb - excitation magnetic flux;
$L_d = L_q$ = 0.03 H - phases inductances;
$X_d = X_q$ = 6.15 Ω - phases reactances;
J = 40 kg m2 - inertia torque
p = 16 - number of poles pair,
R = 1.5 Ω - stator resistance.

### 2.3 Interfacing Power Converters

The considered structure for the electronic conversion system is depicted in figure 3, where the following components can be noticed: wind turbine (WT), permanent magnet synchronous generator (PMSG), diode bridge (DB), hybrid dc-dc converter (HDC), boost voltage inverter (BVI), safety electromechanical brake, Brake load (electrodynamic brake resistor), Supper capacitor and Dump load.

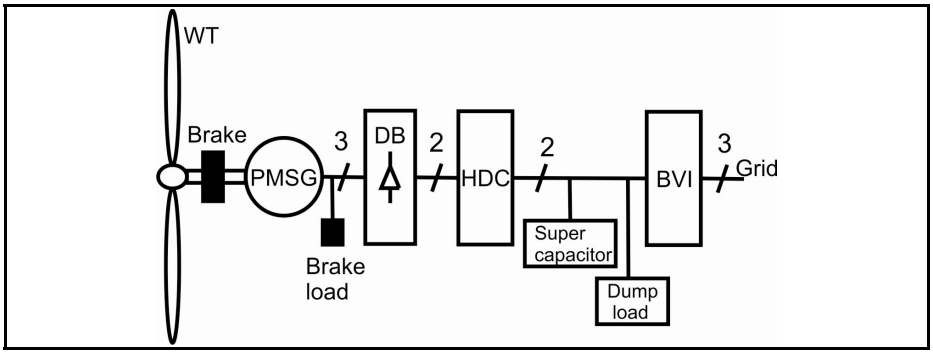


**Fig. 3.** WECS structure

For similar wind generators, many authors proposed new hybrid and Z configurations for dc-dc and dc-ac converters structures, with high voltage gain [4, 5] .

In the considered case, as common solution for low power WECS, the three phase voltage provided by PMSG is rectified by a 6 diodes bridge. The electronic conversion system is based on an intermediary DC circuit with variable voltage, connected between HDC and BVI.

The nominal voltage for super capacitor has to be between 100 and 150 V to assure a low current in the PMSG windings, and increase overall efficiency.

The HDC ratio for input/output voltage is given by (2), considering both economical and technical issues [5,6]:

$$V_{SC} = \frac{D}{2-D} V_{DB} \tag{2}$$

where

$V_{SC}$ - Super Capacitor voltage,
$V_{DB}$ - output voltage of diode bridge,
$D$ - duty cycle.

### 2.4 WECS Braking Systems

For safety reasons, the developed WECS was equipped with three independent braking systems [7] .

The electro-dynamical brake consists of power resistors continuous controlled connected directly to PMSG terminals.

The aero-dynamical brake is integrated in the wind turbine structure, consisting of a centrifugal mechanism able to limit the rotation speed (reducing also the provided power) by modifying the rotor geometry [8] .

The electro-mechanical brake is integrated in the PMSG, consisting of a pair of friction discs electromagnetically actuated provided a braking torque of 450 Nm. This brake is used especially in emergency situations.

## 3 Mathematical Models

### 3.1 Wind Turbine Model

The mathematical model complexity for the considered wind turbine is higher due to the centrifugal protection autonomous system. At various over-speed values the blades adapt their angle in order to change the aerodynamic behavior, decreasing the rotor speed

The estimates based on the mathematical model developed by designers [3,4,9], that take into consideration the blade shape, and turbine architecture, for $\Delta\beta = 0 \ldots 45$ dgr , for the torque coefficient $C_M(v, n, \Delta\beta)$are the following:

$$C_M(v, n, \Delta\beta) = C_{M0\beta}(\Delta\beta) + a_\beta(\Delta\beta)\, \lambda^{\alpha-1}(v, n) - b_\beta(\Delta\beta)\, \lambda^{\beta-1}(v, n) \tag{3}$$

where:

$C_{M0\beta}(\Delta\beta)$ , $a_\beta(\Delta\beta)$, $b_\beta(\Delta\beta)$ expressed as function of angular position of the blades relative to installation position, $\Delta\beta$, are:

$$\begin{aligned} C_{M0\beta}(\Delta\beta) &= (c_{\beta 1} + c_{\beta 2}\, \Delta\beta)/(1 + c_{\beta 3}\, \Delta\beta + c_{\beta 4}\, \Delta\beta^2) \\ a_\beta(\Delta\beta) &= (a_{\beta 1} + a_{\beta 2}\, \Delta\beta^1)/(1 + a_{\beta 3}\, \Delta\beta^1 + a_{\beta 4}\, \Delta\beta^2) \\ b_\beta(\Delta\beta) &= (b_{\beta 1} + b_{\beta 2}\, x)/(1 + b_{\beta 3}\, x + b_{\beta 4}\, x\text{^}2) \end{aligned} \tag{4}$$

The coefficients obtained through linear regression are given in Table 1.

**Table 1.** Linear regression coefficients

| | |
|---|---|
| $c_{\beta 1}$ = 0.012512548 ; | $c_{\beta 2}$ = 0.010797253 ; |
| $c_{\beta 3}$ = 0.04617332 ; | $c_{\beta 4}$ = 9.6420381e-007 . |
| $a_{\beta 1}$ = 0.061078896 ; | $a_{\beta 2}$ = -0.0047310111 ; |
| $a_{\beta 3}$ = -0.0075548307 ; | $a_{\beta 4}$ = -0.00010627525 . |
| $b_{\beta 1}$ = 0.0042482559 ; | $b_{\beta 2}$ = -0.00013577705 ; |
| $b_{\beta 3}$ = -0.09017725 ; | $b_{\beta 4}$ = 0.0038774948 . |

The resulting shaft torque of wind turbine:

$$M_{arb\beta}(v,n,\Delta\beta) = C_{M\beta}(v,n,\Delta\beta)\,\rho\, v^2\, A_v\, R/2 \tag{5}$$

Shaft power coefficient:

$$C_{P\beta}(v,n,\Delta\beta) = C_{M\beta}(v,n,\Delta\beta)\,\lambda(v,n) \tag{6}$$

$$C_{P\beta}(v,n,\Delta\beta) = C_{M0\beta}(\Delta\beta)\;\lambda(v,n) + a_\beta(\Delta\beta)\,\lambda^\alpha(v,n) - b_\beta(\Delta\beta)\,\lambda^\beta(v,n)$$

Shaft power:

$$P_{arb\beta}(v,n,\Delta\beta) = M_{arb\beta}(v,n,\Delta\beta)\,\omega(n)$$

$$P_{arb\beta}(v,n,\Delta\beta) = C_{M\beta}(v,n,\Delta\beta)\,\rho\, v^2\, A_v\, R\,\omega(n)/2 \tag{7}$$

In normal operation the blades angular variation is $\Delta\beta = 0$.

If the rotor speed increases above rated values, the autonomous centrifugal braking system determines a variation of blades angle $0 < \Delta\beta \le 45$.

### 3.2 PMSG Model

The considered PMSG has the following model [10]:

$$\begin{cases} \dfrac{di_d}{dt} = \dfrac{1}{L_d}\left(u_d - Ri_d + p\,\omega_r L_q\, i_q\right) \\ \dfrac{di_q}{dt} = \dfrac{1}{L_q}\left(u_q - Ri_q + p\,\omega_r L_d\, i_d - p\,\omega_r \Phi_f\right) \\ J\dfrac{d}{dt}\omega_r = p\dfrac{1}{J}\left[\dfrac{3}{2}p\left[i_q\Phi_f + \left(L_d - L_q\right)i_d\, i_q\right] + M_m\right] - \dfrac{F}{J}\omega_r \\ \dfrac{d\theta}{dt} = \omega_r \end{cases} \tag{8}$$

Where:

$i_q$, $i_d$ - q and d axes currents,
$v_q$, $v_d$ - q and d axes voltages,
$\omega_r$ - rotor angular speed,
$\Phi_f$ – permanent magnets' flux amplitude,
F = 0.004924 Nm s - total friction coefficient,
$J = J_{WT} + J_{PMSG} = 445 + 40 = 485$ kg m$^2$ – total moment of inertia.

The shaft power $P_m$ corresponding to a given value of generator electric power, can be calculated based on the generator efficiency $\eta_G(n, I_G)$:

$$P_m = P_G / \eta_G \tag{9}$$

In the considered case the efficiency resulted from generator design is:

$$\eta_G(n, I_G) = 4.25\ n\ I_G / (0.09\ I_G^3 + 2.9\ I_G^2 + 4.25\ n\ I_G + 0.075\ n^{1.5}) \tag{10}$$

resulting

$$P_m = F_{pm}(n, I_G) = P_G(n, I_G) / \eta_G(n, I_G) \tag{11}$$

The equation for the wind turbine-generator subsystem, in stationary regime, can be obtained considering the wind turbine power $P_{wt}(n,v)$ and the generator shaft power $P_m(n, I_G)$:

$$P_{wt}(n,v)\ \eta_G(n, I_G) = P_G(n, I_G) \tag{12}$$

## 4 Control of the Wind Energy Conversion System

In order to achieve an efficient control of a WECS, there are necessary good models and characteristics for system components, provided usually by their manufacturer. In our situation, they were not available, and one task prior to develop the control algorithm was to obtain proper models and characteristics, using the developed WECS experimental model. This approach, starting from real data and experimental models was the motivation to refer it as a pragmatic method to design the control strategy.

In normal operating regime (wind power conversion regime), the start-up is validated if the HDC input voltage exceeds a minimum threshold $(U_{HDC})_{input} > (U_{HDC})_{START\ min}$= 190 V assuring the conduction state for the hybrid converter. The no-load phase voltage of PMSG to this threshold is $(U_{PMSG})_{START\ min}$ = 77.86 V, respectively a rotation speed $n_{START\ min}$ = 52 rpm and a wind speed $v_{START\ min}$ = 4.76 m/s. The considered start-up values $(U_{HDC})_{START\ min}$ , $n_{START\ min}$ , $v_{START\ min}$ , were determined experimentally using the ;laboratory modelof WECS .

In diagrams $P_{WT}(v,n)$ and $M_{WT}(v,n)$ presented in Figure 4 – the start-up point is denoted with "a".

The automatic cut-off values $(U_{HDC})_{STOP}$ , $(U_{PMSG})_{STOP}$ , $n_{STOP}$ , $v_{STOP}$ , at small wind speeds, also have been determined on the laboratory model, and are nenoted with “d” in Figure 4.

The WECS nominal regime is determined considering the following physical constraints: the maximal input voltage of HDC, $U_{HDCmax}$ = 380 V and the maximal current for WECS component, in our case $I_{HDCmax}$ = 12.5A.

The experimental tests reveal that above mentioned constraints are accomplished at the rotation speed $n$ = 112 rpm, generator phase voltage $U_{PMSG}$ = 155 V, generator current $I_{PMSG}$ = 12.5A, generator electric power $P_{PMSG}$ = 5400 W, wind speed $v$ = 8.5 m/s (see point “c” in Figure 4). The mentioned operation values will be considered as rated values of WECS [11].

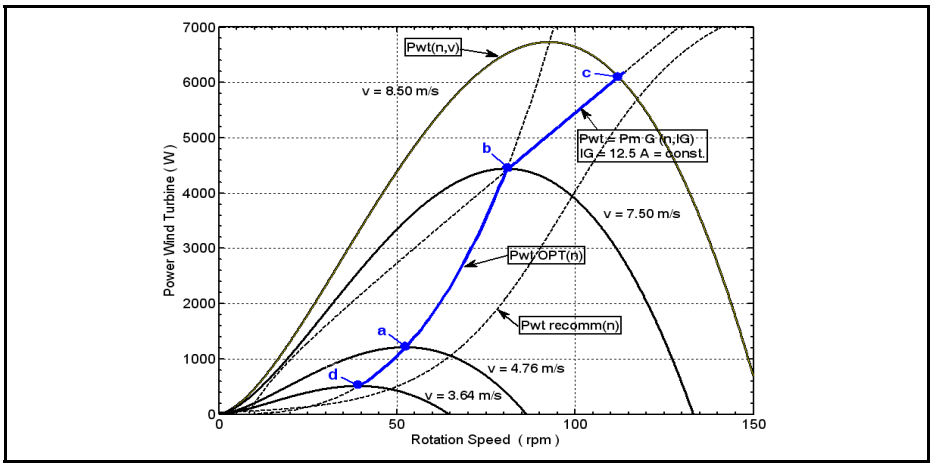


**Fig. 4.** The $P_{WT}$ (v, n), $P_{WT\ opt}$(n) characteristics and the start-up ***a*** and cut-off ***d*** points in energy generating regime

Based on the above considerations it was developed the control strategy for WECS presented in Figure 5.

**S00** represents the state when WT is stopped, and the brake is activated, wind speed being insufficient.

After $\Delta t_1$ (experimental established $\Delta t_1 = 10[\min]$), the system state changes to a waiting state **S10**, releasing the electro-mechanic brake and wait for rotation speed increase.

If after a predefined time, the rotation speed is below the rated value, $\Delta t_2$, $0 < n < n_{START}$, the system returns to **S00**.

If the rotation speed $n > n_{START}$, the system moves to **S20** which represent optimal point functioning.

If the rotation speed decrease below a threshold value $n_{min}$, the system returns to **S10** state.

If the rotation speed exceeds a nominal value $n_{NOM}$, the system enter in the limitation state **S30**, providing the constant current $I_G$. In this case, if the rotation decreases( $n < n_{NOM}$ ) the system returns to S20 state.

If the speed exceeds the maximal value $n_{MAX}$, the system enters the state **S40** corresponding to an extreme operation at high wind speed, when all the braking systems are activated successively: aerodynamically braking through blade rotation angle $0 < \Delta\beta \le \Delta\beta_{MAX}$, electromagnetic braking through current $I_G = I_{G\_ELBRAKE}$, and electro-mechanical braking activation, in order to limit the wind turbine speed in the range $n_{MAX} \le n < n_{EXTREM}$.

The system returns to state S30 if the speed decreases $n < n_{MAX}$.

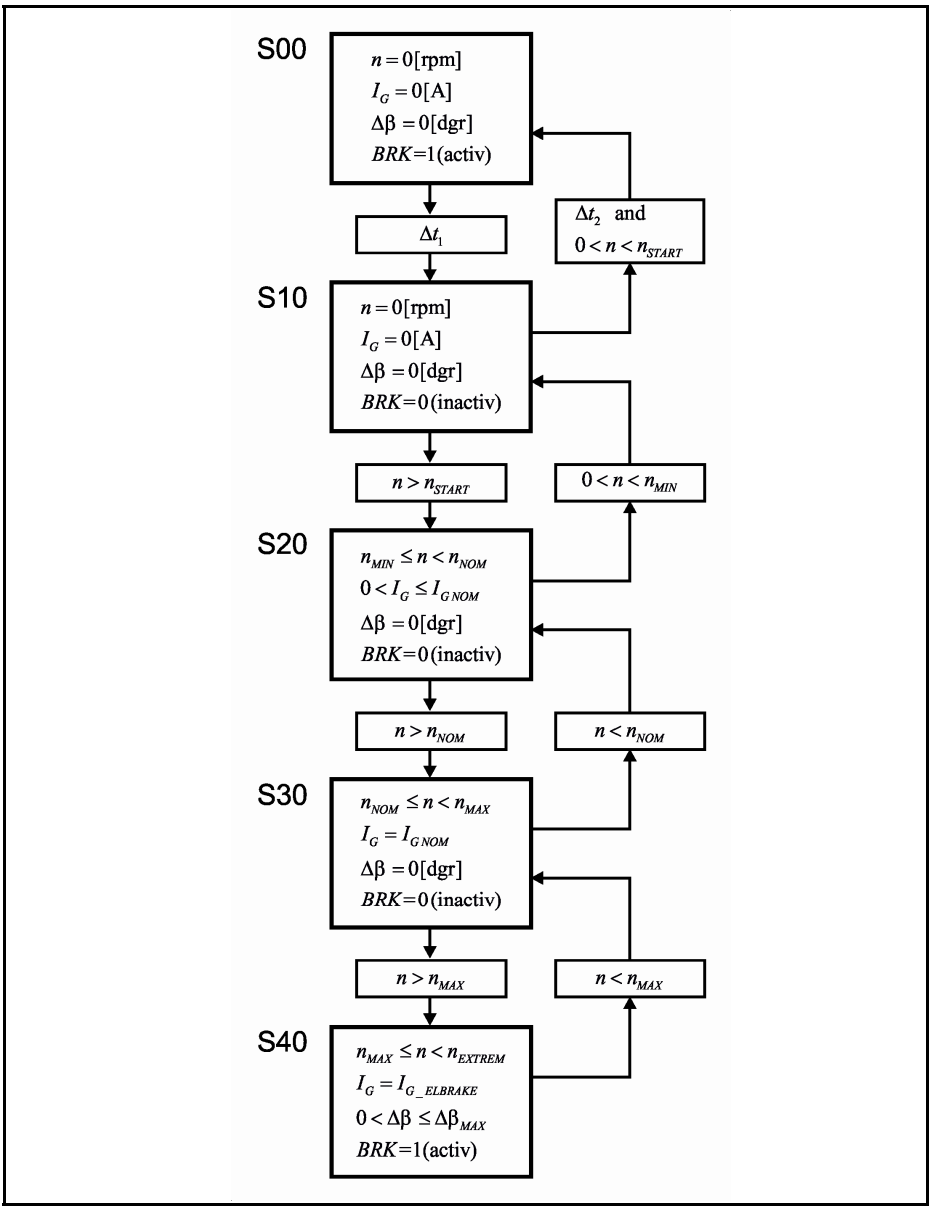


**Fig. 5.** The WECS control algorithm

The aero-dynamical braking system is able to limit the speed $n < n_{EXTREM}$, statement verified at wind speed v = 70 m/s as presented in Figure6.

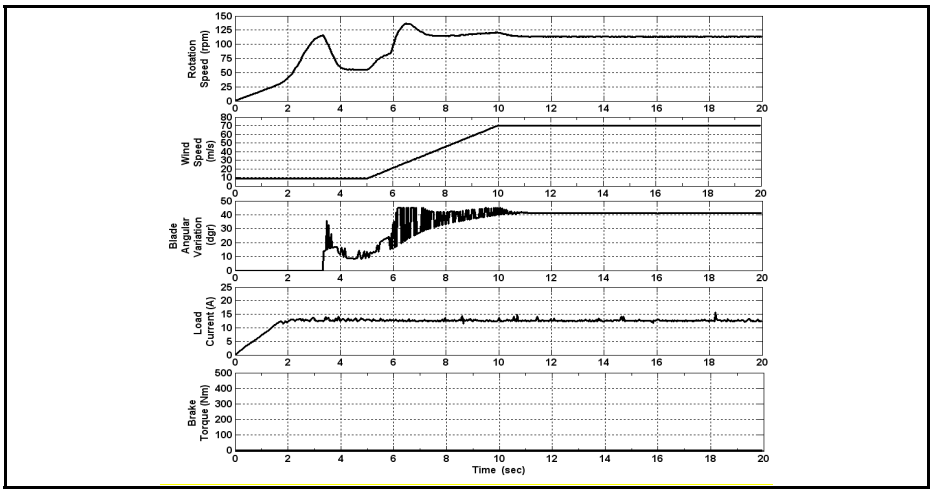


**Fig. 6.** WECS at extreme values of the wind speeds, v = 70 m/s

## 5 Simulation/Experimental Results

The wind turbine characteristic is presented in figure 7, with blades in initial position $\Delta\beta = 0 = \text{const}$. The turbine was designed to provide $P_{WT}(n_{wt}, v)$, even for low wind speed.

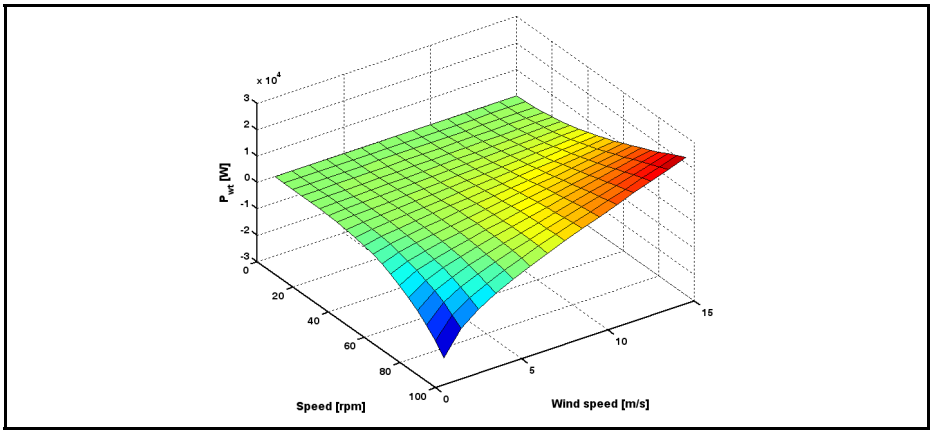


**Fig. 7.** Turbine characteristics $P_{WT}(n_{wt}, v)$ for $\Delta\beta = 0$.

At high rotation speed, and blade position $\Delta\beta = \Delta\beta_{MAX} = 45$ dgr, the turbine presents high aero-dynamical braking torque, as depicted in figure 8.

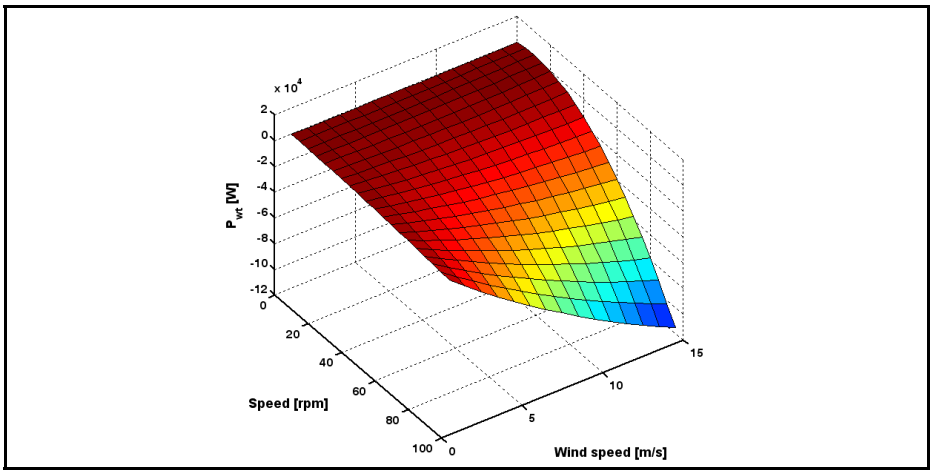


**Fig. 8.** Turbine characteristics $P_{WT}(n_{wt}, v)$ for $\Delta\beta = 45$

The power provided by wind turbine, at constant wind speed v = 8 m/s, in function of rotation speed and angle $\Delta\beta$ is presented in Figure 9.

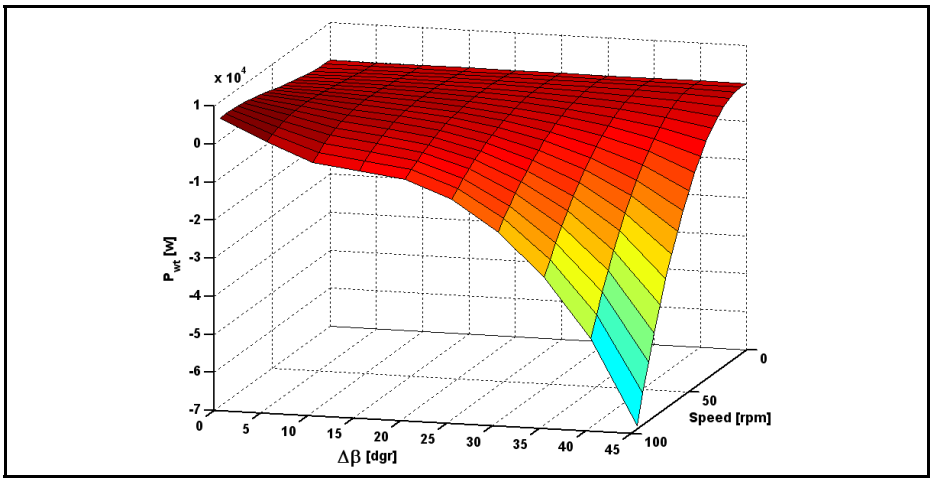


**Fig. 9.** Turbine characteristics $P_{WT}(n_{wt}, v)$ for $\Delta\beta = 0 \ldots 45$.

The wind turbine power curve for the optimal regime $P_{WT\_Opt}(n)$ and respectivelly the equivalent shaft power $P_{WT}(n)$, for a number of $N_{point} = 10279$ measurements during the operating regime is depicted in Figure 10. The considered efficiency of the PMSG is $\eta_{PMSG} = 91\%$.

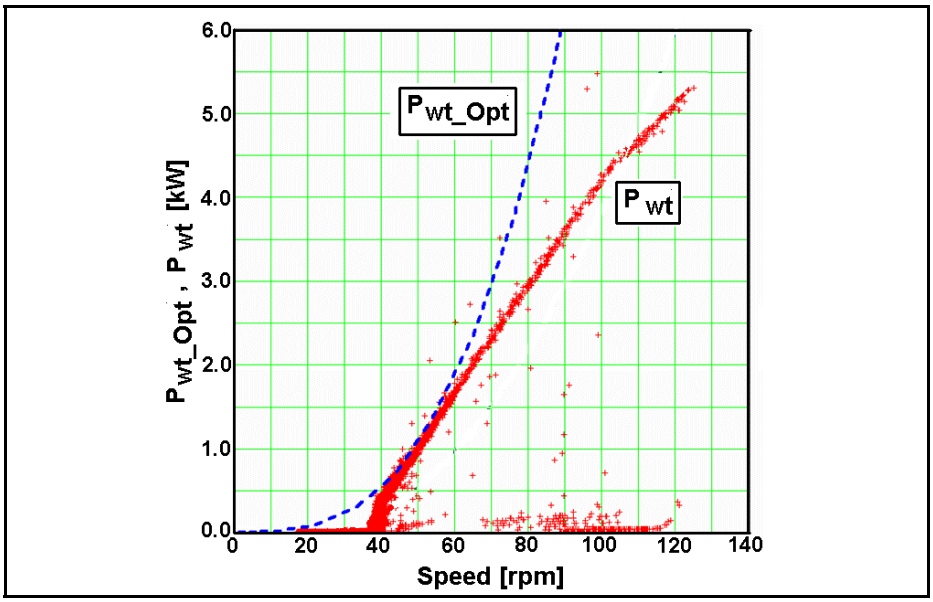


**Fig. 10.** Optimal regime power $P_{WT\_Opt}(n)$ and equivalent shaft power $P_{WT}(n)$

There can be noticed that shaft power distribution corresponds to reference curve of WECS. The power conversion is started at a rotation speed of 40 rpm and the functioning in optimal regime along $P_{WT\_Opt}(n)$ curve (with an insignificant deviation) is until 80 rpm, followed by a constant current regime limited at $I_G$ = 12.5 A for speeds above 80 rpm.

## 6 Conclusions

The studies performed on the laboratory models confirmed the hypothesis adopted in designing the WECS and its elements.

The control algorithm in different operation regimes (nominal or faulty) has been also confirmed, through the experimental tests on the developed laboratory model, complying all conditions imposed by the present-day standards in the domain of WECS [12].

## References

1. Chen, Z., Guerrero, J.M., Blaabjerg, F.: A review of the state of the art of power electronics for wind turbines. IEEE Trans. Power Electr. 24(8), 1859–1875 (2009)
2. Muntean, N., Cornea, O., Petrila, D.: A New Conversion and Control System for a Small Off – Grid Wind Turbine. In: 12th International Conference on Optimization of Electrical and Electronic Equipment, OPTIM 2010, pp. 1167–1173. IEEE (2010); 978-1-4244-7020

3. Milos, T., Gyulai, F.: CAD technique for blade design of small power wind turbine. In: Proceedings of the International Conference on Hydraulic Machinery and Equipments, HME 2008, Timisoara, Romania (2008)
4. Peng, F.Z.: Z-source inverter. IEEE Trans. Ind. Applic. 39, 504–510 (2003)
5. Axelrod, B., Berkovich, Y., Ioinovici, A.: Switched-capacitor/ switched inductor structures for getting transformer less hybrid dc-dc PWM converters. IEEE Trans. Circ. and Syst. 55(2), 687–696 (2008)
6. Gao, F., Loh, P.C., Teodorescu, R., Blaabjerg, F.: Diode assisted buck boost voltage source inverters. IEEE Trans. Power Electr. 24(9), 2057–2064 (2009)
7. Koch-Ciobotaru, C., Boraci, R., Filip, I., Vasar, C.: Study of brake transient regimes for a small wind generator. In: IEEE 3rd International Symposium on Exploitation of Renewable Energy Sources (EXPRES), March 11-12, pp. 85–89 (2011)
8. Milos, T., Bej, A., Dobanda, E., Manea, A., Badarau, R., Stroita, D.: Blade design using CAD technique for small power wind turbine. In: International Joint Conference on Computational Cybernetics and Technical Informatics (ICCC-CONTI), Timisoara, Romania, May 27-29, pp. 571–575 (2010)
9. Babescu M.: Electrical machines. The ortogonal model. Publishing House Politehnica, Timisoara (2000)
10. Koch-Ciobotaru, C., Boraci, R., Prostean, O., Budisan, N.: Optimal control for a variable-speed wind turbine. In: 6th IEEE International Symposium on Applied Computational Intelligence and Informatics (SACI), May 19-21, pp. 541–544 (2011)
11. Boraci, R., Koch-Ciobotaru, C., Protean, O., Budisan, N.: Experimental determination of an optimal control law of a small windgenerator. In: IEEE 6th IEEE International Symposium on Applied Computational Intelligence and Informatics (SACI), May 19-21, pp. 545–548 (2011)
12. International Standard IEC 614000-2, Part.2: Design requirements for small wind turbines